Optical Engineering 44(10), 105801 (October 2005)

Applicability of time-average fluid holography for analysis of propagating waves

Minvydas Ragulskis
Kaunas University of Technology
Department of Mathematical Research in Systems
Studentu 50-222
Kaunas, Lithuania
E-mail: Minvydas.Ragulskis@ktu.LT

Arvydas Palevicius, MEMBER SPIE
Kaunas University of Technology
International Studies Center
Mickeviciaus 37
Kaunas, Lithuania

Algimantas Fedaravicius
Kaunas University of Technology
Department of Mechanical Engineering
Kestucio 27
Kaunas, Lithuania

Liutauras Ragulskis
Vytautas Magnus University
Department of Informatics
Vileikos 8
Kaunas, Lithuania

Abstract. Numerical procedures for construction of digital patterns of fringes mimicking fluid holograms are developed. Because conventional finite-element fluid analysis techniques are based on the approximation of nodal displacements, conjugate smoothing of the values of volumetric strain is performed in order to obtain realistic holographic images. Two-dimensional fluid oscillations are analyzed using the developed techniques. It is shown that though time-average fluid holography is a powerful optical experimental method for analysis of short-term transient processes and harmonic vibrations, it has rather limited applicability to studying propagating waves. © *2005 Society of Photo-Optical Instrumentation Engineers.* [DOI: 10.1117/1.2080747]

Subject terms: finite-element method; time-average holography; volumetric strain; propagating wave.

Paper 040826R received Nov. 4, 2004; revised manuscript received Mar. 1, 2005; accepted for publication Mar. 18, 2005; published online Oct. 4, 2005.

1 Introduction

Development of hybrid numerical-experimental techniques is an important engineering analysis method used for interpretation and validation of experimental results.[1,2] Such techniques are of high importance when physical processes taking place in the analyzed systems are complex and it is hard to expect that produced results could be directly deduced even by experienced investigators. A typical example is time-average optical holography,[3,4] where the inverse problem of motion reconstruction from the pattern of interference fringes is often an ill-posed problem and does not have unique solutions if the motion of the analyzed structures was not harmonic.[5]

A method of mimicking patterns of fringes corresponding to experimental time-average fluid holograms is presented in this paper. Moreover, this numerical visualization technique is used to study the applicability of time-average fluid holography for analysis of traveling waves.

For simplicity two-dimensional fluid vibrations are considered only. This does not imply that the proposed technique can be applied only for 2-D analysis. On the other hand, there exist many important engineering problems where 2-D fluid-structure interaction problems are of even higher importance than 3-D problems. A typical example is discussed in Ref. 6, where a traveling fluid wave carries a thin film of elastic material.

Laser holography is a powerful experimental technique for analysis of high-frequency structural vibrations, especially when the amplitudes of those vibrations are relatively small.[3] It is a nondestructive whole-field optical method, successfully applied to the analysis of fluid motion also.[7] Nevertheless, an open question remains whether time-average laser holography can be applied to the analysis of propagating waves in fluids. That question is very important for such systems as are described in Ref. 6. The answer to that question is sought by building numerical models of the fluid, calculating volumetric strains, and developing digital image reconstruction techniques based on optical-holography physical relationships.

The construction of the digital holographic image consists of three stages:

1. calculations using the displacement formulation by the method of finite elements described in Sec. 2
2. determination of the field of volumetric strain as described in Sec. 4
3. construction of the digital holographic image as described in Sec. 3.

2 Finite-Element Model of the System

The numerical model for the irrotational motions of a two-dimensional ideal compressible fluid with a free surface is developed using the finite-element method (FEM).[8–10] It is based on the principle of virtual displacements with the

condition of irrotationality taken into account by the penalty method. The mass matrix of the fluid is

$$\mathbf{M} = \int \mathbf{N}^T \rho_0 \mathbf{N} \, dx \, dy, \tag{1}$$

where ρ_0 is the density of the fluid in equilibrium; x is the longitudinal coordinate; y is the vertical coordinate; $\mathbf{N}$ is the matrix of the shape functions defined by the relationship

$$\begin{Bmatrix} u \\ v \end{Bmatrix} = \mathbf{N}\boldsymbol{\delta}, \tag{2}$$

where u, v denote fluid displacements in the directions of the x and y axes in the domain of appropriate finite elements; and $\boldsymbol{\delta}$ is the nodal fluid displacement vector. Explicitly,

$$\mathbf{N} = \begin{bmatrix} N_1 & 0 & N_2 & 0 & \cdots \\ 0 & N_1 & 0 & N_2 & \cdots \end{bmatrix}, \tag{3}$$

where N_i are the shape functions of the analyzed finite element. The stiffness matrix of the fluid, taking the condition of irrotationality into account by the penalty method, is constructed in the following way:

$$\mathbf{K} = \int (\bar{\mathbf{B}}^T \rho_0 c^2 \bar{\mathbf{B}} + \tilde{\mathbf{B}}^T \lambda_0 \tilde{\mathbf{B}}) \, dx \, dy + \int \bar{\mathbf{N}}^T \rho_0 g \bar{\mathbf{N}} \, dx, \tag{4}$$

where c is the speed of sound in the fluid, λ_0 the penalty parameter for the condition of irrotationality,[9] and g the acceleration of gravity. It can be noted that the second integral is calculated over the free surface only (along the x axis). The matrix $\bar{\mathbf{B}}$ relating the volumetric strain to the displacements is defined from

$$\frac{\partial u}{\partial x} + \frac{\partial v}{\partial y} = \bar{\mathbf{B}}\boldsymbol{\delta}. \tag{5}$$

Explicitly,

$$\bar{\mathbf{B}} = \begin{bmatrix} \frac{\partial N_1}{\partial x} & \frac{\partial N_1}{\partial y} & \frac{\partial N_2}{\partial x} & \frac{\partial N_2}{\partial y} & \cdots \end{bmatrix}. \tag{6}$$

The matrix $\tilde{\mathbf{B}}$ is used to characterize the rotation and is defined from

$$\frac{\partial u}{\partial y} - \frac{\partial v}{\partial x} = \tilde{\mathbf{B}}\boldsymbol{\delta}. \tag{7}$$

Thus

$$\tilde{\mathbf{B}} = \begin{bmatrix} \frac{\partial N_1}{\partial y} & -\frac{\partial N_1}{\partial x} & \frac{\partial N_2}{\partial y} & -\frac{\partial N_2}{\partial x} & \cdots \end{bmatrix}. \tag{8}$$

The matrix $\bar{\mathbf{N}}$ of the shape functions is used to characterize the motion of the free surface of the fluid and is defined from the following relationship:

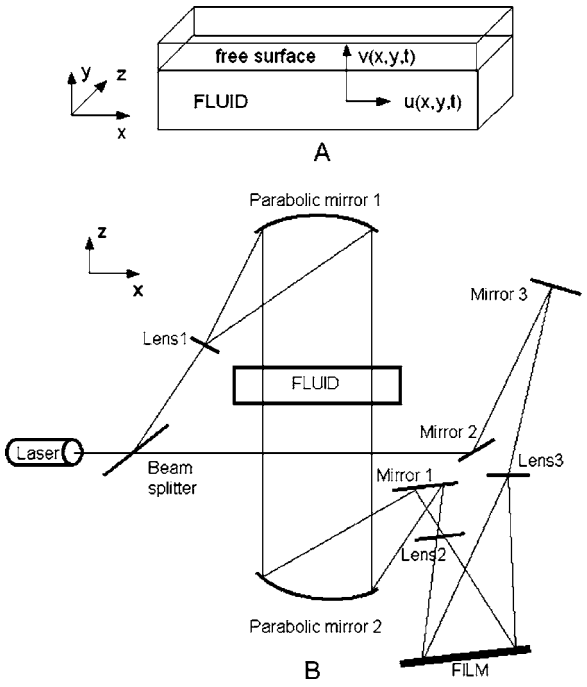

Fig. 1 Schematic diagram of the experimental setup: (a) geometry of the fluid bath; (b) optical setup.

$$v = \bar{\mathbf{N}}\boldsymbol{\delta}, \tag{9}$$

where

$$\bar{\mathbf{N}} = [0 \quad N_1 \quad 0 \quad N_2 \quad \cdots]. \tag{10}$$

The global mass and stiffness matrices of the fluid are constructed by applying the classical direct stiffness method[10] over the global domain.

3 Numerical Procedure for the Construction of the Digital Holographic Image

A schematic diagram of the experimental setup is shown in Fig. 1. A beam from a laser is split into two beams by a beamsplitter, forming the object and the reference beams. The object beam is collimated by spherical lens 1 and parabolic mirror 1 before passing through the investigated fluid. After passing it, the diameter of the beam is reduced by the combination of parabolic mirror 2 and spherical lens 2. They image the investigated fluid onto the holographic film. The reference beam passes through mirrors 2 and 3 and then is expanded by lens 3. It illuminates the holographic film, interfering with the object beam. Time averaging in the analysis of vibrations by holographic methods is presented in detail in Ref. 3. A digital numerical procedure is used for the construction of the digital image. The following development is necessary for the construction of the digital holographic image from the results of finite-element calculations.

The phase of the light from the laser beam $\Psi(x,y,t)$ can be expressed as[7]

$$\Psi(x,y,t) = \frac{2\pi}{\lambda}[n_0 - n_{\text{flow}}(x,y,t)]h, \tag{11}$$

where h is the distance that the light travels through the fluid, λ the wavelength of the laser beam, and n_0 and $n_{\text{flow}}(x,y,t)$ the refractive indices in the initial and flow conditions, respectively.

The refractive index is expressed as[7]

$$n(x,y,t) = 1 + \beta\frac{\rho(x,y,t)}{\rho_0}, \tag{12}$$

where ρ_0 is the density (constant in the region of the flow in equilibrium), β the constant of proportionality, and $\rho(x,y,t)$ is the density of the fluid. In our case from this equation it follows that $n_0 = 1+\beta$ and $n_{\text{flow}}(x,y,t) = 1 + \beta\rho_{\text{flow}}(x,y,t)/\rho_0$. From previous relationships and Eq. (11) it follows that

$$\Psi(x,y,t) = \Psi_0 - k\rho_{\text{flow}}(x,y,t), \tag{13}$$

where the initial phase Ψ_0 and the coefficient of proportionality k are expressed as

$$\Psi_0 = \frac{2\pi}{\lambda}\beta h, \tag{14}$$

$$k = \frac{2\pi}{\lambda}\frac{\beta}{\rho_0}h. \tag{15}$$

The deviation of the fluid density from its value in equilibrium is denoted as

$$\tilde{\rho}(x,y,t) = \rho_{\text{flow}}(x,y,t) - \rho_0. \tag{16}$$

It is assumed that this deviation is small. This is a natural assumption, keeping in mind that standard FEM models are built around the equilibrium state. Thus

$$|\tilde{\rho}(x,y,t)| \ll \rho_0. \tag{17}$$

Then the phase on the basis of Eqs. (13) and (16) can be expressed as

$$\Psi(x,y,t) = \overline{\Psi_0} - k\tilde{\rho}(x,y,t), \tag{18}$$

where

$$\overline{\Psi_0} = \Psi_0 - k\rho_0. \tag{19}$$

These relationships enable numerical reconstruction of the laser-beam light phase in the liquid flow. Our analysis is concentrated on propagating waves in fluids; therefore it is assumed that the density and the displacements of the fluid are harmonically varying in time. Thus the fields of density and displacements can be simplified to the form

$$\rho_{\text{flow}}(x,y,t) = \rho_0 + \tilde{\rho}^*(x,y)\cos\omega t \tag{20}$$

and

$$u(x,y,t) = \tilde{u}^*(x,y)\sin\omega t,$$

$$v(x,y,t) = \tilde{v}^*(x,y)\sin\omega t, \tag{21}$$

where the angular frequency ω coincides with the natural frequency of oscillation of the appropriate eigenmode, $\tilde{\rho}^*(x,y)$ is the eigenmode of the variation of the density, and $\tilde{u}^*(x,y), \tilde{v}^*(x,y)$ are the eigenmodes of the displacements.

The condition of the continuity of the fluid[8] when the condition given by Eq. (17) is valid can be represented as

$$\frac{\partial\rho_{\text{flow}}}{\partial t} = -\rho_0\left(\frac{\partial u}{\partial x} + \frac{\partial v}{\partial y}\right). \tag{22}$$

Equation (22) together with the Eqs. (20) and (21) yields

$$\tilde{\rho}^*(x,y)\omega = \rho_0\left[\frac{\partial\tilde{u}^*(x,y)}{\partial x} + \frac{\partial\tilde{v}^*(x,y)}{\partial y}\right]. \tag{23}$$

Time averaging is advantageous for the analysis of high-frequency vibrations. The arrangement and illumination used in time-averaged holography are described in detail in Ref. 3. The resulting intensity of illumination in the hologram obtained by using the method of time averaging[3] is proportional to the volumetric strain and can be expressed as[3,7]

$$I = \lim_{T\to\infty}\left\{\int_0^T \frac{1}{T}\left|\exp\left[ja\left(\frac{\partial u(x,y,t)}{\partial x} + \frac{\partial v(x,y,t)}{\partial y}\right)\right]\right| \mathrm{d}t\right\}^2, \tag{24}$$

where T is the exposure time, j is the imaginary unit, and a is a coefficient proportional to the intensity of the laser beam in the hologram plane. From the equations (18) and (23),

$$a = -\frac{k\rho_0}{\omega}. \tag{25}$$

If the variation of the volumetric strain is harmonic and the exposure time is much longer than the period of oscillation, the expression in Eq. (24) converges to

$$I = J_0^2\left(a\left(\frac{\partial\tilde{u}^*(x,y)}{\partial x} + \frac{\partial\tilde{v}^*(x,y)}{\partial y}\right)\right), \tag{26}$$

where J_0 is the zero-order Bessel function of the first kind. Note that the frequency of oscillations will have no effect on the pattern of fringes, and the centers of dark fringes will coincide with the roots of the Bessel function. The numerical procedures for developing approximate iterative formulas for computing of values of the Bessel function and brightening the produced image are presented explicitly in Ref. 11. Moreover, if the analyzed fluid performs harmonic vibrations, it is enough to evaluate only the cosine part of the integral in Eq. (24), for the imaginary sine part of the integral converges to zero.

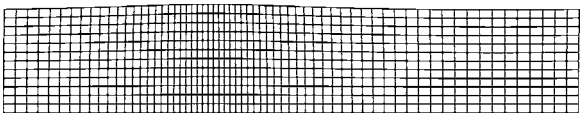

Fig. 2 FEM meshing in the global domain distorted according to the second eigenmode.

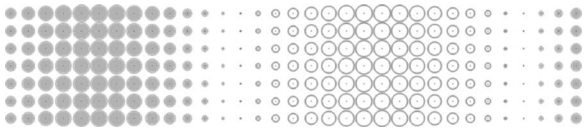

Fig. 3 Nodal volumetric strains for the second eigenmode.

A propagating wave in a fluid can be interpreted as a superposition of two multiple eigenmodes in a periodic system:

$$u(x,y,t) = F_1^u(x,y)\sin\omega t + F_2^u(x,y)\cos\omega t,$$
$$v(x,y,t) = F_1^v(x,y)\sin\omega t + F_2^v(x,y)\cos\omega t, \tag{27}$$

where $u(x,y,t)$ and $v(x,y,t)$ are displacements, F_1 and F_2 are the multiple eigenmodes, superscripts denote directions, and ω is eigenfrequency. Thus,

$$\frac{\partial u}{\partial x}+\frac{\partial v}{\partial y} = \left(\frac{\partial F_1^u}{\partial x}+\frac{\partial F_1^v}{\partial y}\right)\sin\omega t + \left(\frac{\partial F_2^u}{\partial x}+\frac{\partial F_2^v}{\partial y}\right)\cos\omega t. \tag{28}$$

Keeping in mind that modern time-average holographic techniques enable production of holographic images with short exposure times,[5] the intensity of illumination can be calculated for fractional parts of the period of oscillation, but in that case both sine and cosine parts of the integral must be evaluated.

4 Conjugate Approximation of Volumetric Strain

Conventional FEM analysis techniques are based on the approximation of nodal displacements via the shape functions.[10,12] But volumetric strains (not nodal displacements) are involved in the relationships governing the intensity of illumination in the hologram plane. In turn, volumetric strains are calculated as partial derivatives of displacements. The fields of displacements in the global domain are continuous. But the field of volumetric strains due to the operation of differentiation is continuous in the domains of individual elements but discontinuous at interelement boundaries. Thus a special procedure of smoothing of the field of volumetric strain in the global domain must be developed in order to produce smooth patterns of fringes. This technique is developed on the basis of conjugate approximation with smoothing, which was proposed for the smoothing of the components of stresses in Ref. 13.

First the volumetric strains at the points of numerical integration of the finite element are calculated in the usual way:

$$\frac{\partial u}{\partial x}+\frac{\partial v}{\partial y} = \bar{\mathbf{B}}\boldsymbol{\delta}_0, \tag{29}$$

where $\boldsymbol{\delta}_0$ is the vector of nodal displacements of the eigenmode, and $\bar{\mathbf{B}}$ is the matrix relating the volumetric strains to the displacements given by Eq. (6). The eigenmode of strains is obtained by minimizing the following augmented residual:

$$\frac{1}{2}\int\int\left([\mathbf{N}\boldsymbol{\delta}_v-(u_x+v_y)]^2+\mu\left\{\left[\frac{\partial(u_x+v_y)}{\partial x}\right]^2+\left[\frac{\partial(u_x+v_y)}{\partial y}\right]^2\right\}\right)\mathrm{d}x\,\mathrm{d}y, \tag{30}$$

where μ is the smoothing parameter; $\boldsymbol{\delta}_v$ the vector of nodal values of $\partial u/\partial x+\partial v/\partial y$ (the eigenmode of volumetric strains), and $\mathbf{N}$ the row matrix of the shape functions of the finite element:

$$\mathbf{N} = [N_1 \quad N_2 \quad \cdots \quad N_n]. \tag{31}$$

The augmented term takes the following form:

$$\left[\frac{\partial(u_x+v_y)}{\partial x}\right]^2+\left[\frac{\partial(u_x+v_y)}{\partial y}\right]^2 = \boldsymbol{\delta}_v^T\mathbf{B}^{*T}\mathbf{B}^*\boldsymbol{\delta}_v, \tag{32}$$

where $\mathbf{B}^*$ is the matrix of the derivatives of the shape functions:

$$\mathbf{B}^* = \begin{bmatrix} \frac{\partial N_1}{\partial x} & \frac{\partial N_2}{\partial x} & \cdots & \frac{\partial N_n}{\partial x} \\ \frac{\partial N_1}{\partial y} & \frac{\partial N_2}{\partial y} & \cdots & \frac{\partial N_n}{\partial y} \end{bmatrix}. \tag{33}$$

Step-by-step differentiation leads to the following system of linear-algebraic equations for the determination of smoothed volumetric strains:

$$\int\int(\mathbf{N}^T\mathbf{N}+\mathbf{B}^{*T}\mu\mathbf{B}^*)\mathrm{d}x\mathrm{d}y\cdot\boldsymbol{\delta}_v = \int\int\mathbf{N}^T\left(\frac{\partial u}{\partial x}+\frac{\partial v}{\partial y}\right)\mathrm{d}x\,\mathrm{d}y. \tag{34}$$

The choice of the smoothing parameter is performed on the basis of mean finite-element error norms. Their determination requires us to solve the previously described system of linear algebraic equations for the determination of the nodal volumetric strains with $\mu=0$. The volumetric strain $\varepsilon_v=\partial u/\partial x+\partial v/\partial y$ can be interpolated from its nodal values by using the shape functions of the finite element. Further, ε_v denotes the values obtained by using this interpolation. The relative error norm for the i'th finite element can be calculated as

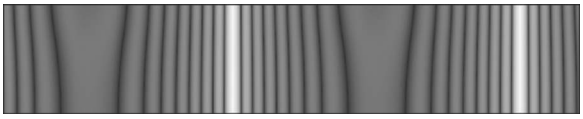

Fig. 4 Smoothed time-average holographic interferogram for the second eigenmode.

$$\psi_i = \frac{\int\int_{e_i} (\varepsilon_v - \bar{\mathbf{B}}\boldsymbol{\delta}_0)\rho_0 c^2 (\varepsilon_v - \bar{\mathbf{B}}\boldsymbol{\delta}_0)\, \mathrm{d}x\, \mathrm{d}y}{\int\int_{e_i} \varepsilon_v \rho_0 c^2 \varepsilon_v\, \mathrm{d}x\, \mathrm{d}y}. \tag{35}$$

Thus the obtained field of volumetric strain is used in the construction of the digital holographic image as described in the previous section.

5 Numerical Results

A two-dimensional free-surface fluid in a rectangular periodic domain is analyzed. The lower boundary is rigid, and the displacements normal to it are set to zero. The upper surface is assumed to be free. Periodic boundary conditions in the x direction are assumed—the values of the displacements on the left and the right boundaries at same y coordinate are assumed to be equal. The second eigenmode of the fluid is shown in Fig. 2.

Nodal values of volumetric strain corresponding to the second eigenmode are presented in Fig. 3. Note that the values are shown only for every second node in both directions. The absolute magnitude of the volumetric strain is directly proportional to the radius of the circle; positive values correspond to empty circles; negative values, to full gray circles.

The smoothed images for the second and third eigenmodes are shown in Fig. 4 and Fig. 5. It can be noted that the two eigenmodes are multiple (same eigenfrequency). The procedure for construction of digital images in the virtual projection plane is described in detail in Ref. 11.

The propagating wave in the analyzed domain is constructed as a superposition of the second and the third eigenmodes as described in Eq. (27). Numerical results are presented in Fig. 6. It can be noted that when the exposure time increases, the digital image gets blurred and converges to a gray, uninterpretable image. On the other hand, the direction of wave propagation can be clearly inferred from the sequence of the images presented in this figure, though quantitative determinations would require more sophisticated analytical developments and are beyond the scope of this research. Finally, when the exposure time tends to infinity, the interference fringes are averaged to a uniform gray image. One should keep in mind that the exposure time of the whole period on the basis of Eq. (24) gives the same result as the exposure time tending to infinity. This is because for periodic motion the average over a period is equal to the average over many periods.

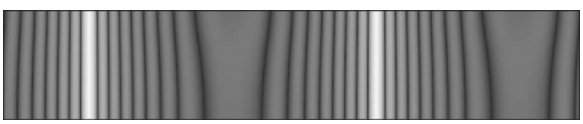

Fig. 5 Smoothed time-average holographic interferogram for the third eigenmode.

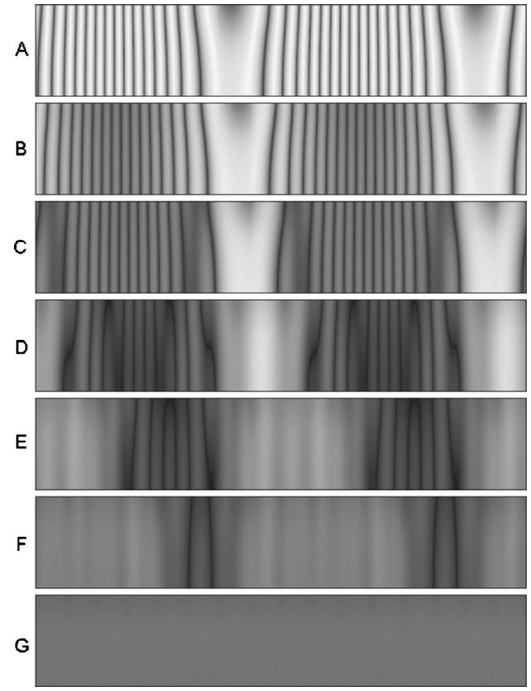

Fig. 6 The smoothed digital time-averaged holographic image of the traveling wave: exposure time (a) 1/64 period; (b) 1/32 period; (c) 1/16 period; (d) 1/8 period; (e) 1/4 period; (f) 3/4 period; (g) 1 period.

6 Conclusions

A numerical method for the construction of digital time-averaged fluid holographic images has been developed. The obtained time-averaged holographic images can be effectively used for investigation of oscillatory motions in fluid transport systems. It is shown that time-average fluid holography has limited applicability for analysis of propagating waves unless sufficiently short exposure times are used. Of course, it is difficult to expect more, but even the obtained results provide background for the analysis of fluid motions.

References

1. A. Holstein, L. Salbut, M. Kujawinska, and W. Juptner, "Hybrid experimental–numerical concept of residual stress analysis in laser weldments," *Exp. Mech.* **41**(4), 343–350 (2001).
2. M. Ragulskis and L. Ragulskis, "Plotting isoclinics for hybrid photoelasticity and finite element analysis," *Exp. Mech.* **44**(3), 235–240 (2004).
3. C. M. Vest, *Holographic Interferometry*, Wiley, New York (1979).
4. P. K. Rastogi, "Principles of holographic interferometry and speckle metrology," *Top. Appl. Phys.* **77**, 103–150 (2000).
5. M. A. Caponero, P. Pasqua, A. Paolozzi, and I. Peroni, "Use of holographic interferometry and electronic speckle pattern interferometry for measurements of dynamic displacements," *Mech. Syst. Signal Process.* **14**(1), 49–62 (2000).
6. M. Ragulskis and K. Koizumi, "Applicability of attractor control techniques for a particle conveyed by a propagating wave," *J. Vib. Control* **10**(7), 1057–1070 (2004).
7. A. Houwing, K. Takayama, K. Koremoto, T. Hashimoto, and H. Mitobe, "Finite fringe analysis of two dimensional and axially-symmetric flows," *Proc. SPIE* **398**, 174–180 (1983).

8. N. F. Iershov and G. G. Shahvierdi, *The Method of Finite Elements in the Problems of Hydrodynamics and Hydroelasticity*, Sudostroienie, Leningrad (1984).
9. J. Eibl, and L. Stempniewski, "Dynamic analysis of liquid filled tanks including plasticity and fluid interaction—earthquake effects," in *Shell and Spatial Structures: Computational Aspects, Proc. Int. Symp.*, pp. 261–269, Springer-Verlag, Berlin (1987).
10. L. J. Segerlind, *Applied Finite Element Analysis*, Mir, Moscow (1979).
11. M. Ragulskis, A. Palevicius, and L. Ragulskis, "Plotting holographic interferograms for visualisation of dynamic results from finite element calculations," *Int. J. Numer. Methods Eng.* **56**(11), 1647–1659 (2003).
12. S. S. Rao, *The Finite Element Method in Engineering*, Pergamon Press, Oxford (1982).
13. M. Ragulskis and L. Ragulskis, "Conjugate approximation with smoothing for hybrid photoelastic and FEM analysis," *Commun. Numer. Methods Eng.* **20**(8), 647–653 (2004).

Minvydas Ragulskis received his PhD degree in 1992 from Kaunas University of Technology, Lithuania, and is currently a professor in the Department of Mathematical Research in Systems. His research interests are numerical analysis and nonlinear dynamics.

Arvydas Palevicius received his PhD degree in 1985 from Kaunas University of Technology, Lithuania, where he has been with the Vibrotechnika Research Center since 1999, and is currently a professor in the Department of International Studies, Kaunas University of Technology. His research interests are laser holographic interferometry and microlithography.

Algimantas Fedaravicius received his PhD degree in 1979 from Kaunas University of Technology, Lithuania, where he has been with the Vibrotechnika Research Center, and is currently a professor and dean in the Department of Mechanical Engineering, Kaunas University of Technology. His research interests are dynamics of electromechanical systems and mechatronics.

Liutauras Ragulskis received his PhD degree in 1987 from Kaunas University of Technology, Lithuania. He has been with Lithuanian Institute of Energy since 1988 and at Vytautas Magnus University since 1991, where he is currently a research associate in the Department of Informatics. His research interests are programming and application of finite-element methods.